Performance Measurement of Shock-Induced Fluidic Thrust Vector Control in a Dual-Bell Nozzle

Anis Tcherak
Aeronautical Sciences Laboratory, Institute of Aeronautics and Space Studies
University of Blida 1
Blida, Algeria
tcherak_anis@univ-blida.dz

Hakim Kbab
Aeronautical Sciences Laboratory, Institute of Aeronautics and Space Studies
University of Blida 1
Blida, Algeria
kbab_hakim@univ-blida.dz

Amine Tcherak
LRDSI, Dept. Computer Science
University of Blida 1
Blida, Algeria
tcherak_amine@univ-blida.dz

Abdelkrim Haddad
Applied Mechanics of New Materials Laboratory LMANM, Mechanical Engineering Department
Université 8 Mai 1945
Guelma, Algeria
haddad.abdelkrim@guelma-univ.dz

***Abstract*—Dual-bell nozzle (DBN) is an altitude-adaptive rocket nozzle concept that improves performance over a wide range of operating conditions. In parallel, fluidic thrust vector control has emerged as a promising alternative to conventional mechanical systems by enabling thrust deflection through controlled manipulation of the internal flow field. In this study, the performance of shock-induced fluidic thrust vector control applied to a DBN configuration is investigated. The analysis is conducted on an innovative subscale DBN designed using an in-house developed method of characteristics (MoC) code, with the resulting geometry subsequently validated through computational fluid dynamics (CFD) simulations. Thrust vectoring is achieved through secondary flow injection, which generates asymmetric shock structures and controlled flow separation within the nozzle. The resulting pressure redistribution produces a lateral force component leading to thrust deflection. The performance of the proposed configuration is evaluated in terms of thrust vector angle, pressure distribution, and vectoring efficiency. The results demonstrate that shock-induced fluidic control enables effective thrust vectoring while preserving the stable flow separation characteristics associated with dual-bell operation. These findings provide further insight into the interaction between shock dynamics and fluidic actuation, highlighting the potential of this approach for future rocket propulsion systems requiring efficient and lightweight thrust vector control solutions.**

Keywords—Dual-bell nozzle (DBN), Fluidic thrust vector control, Method of characteristics (MoC), Computational fluid dynamics (CFD)

I. INTRODUCTION

In contemporary rocket propulsion systems, the nozzle is a critical component that directly influences engine efficiency and overall vehicle performance. Among advanced nozzle configurations, the dual-bell nozzle (DBN) has attracted considerable interest due to its inherent capability to adapt passively to variations in ambient pressure. This altitude-compensating feature allows the nozzle to maintain efficient thrust generation over a broad range of flight conditions, thereby enhancing payload capacity and operational flexibility for launch vehicles [1].

Originally proposed by Cowles et al. [2] in 1949, the DBN geometry is characterized by two successive divergent sections connected through an inflection point, as illustrated in Fig. 1. The first section, commonly referred to as the base nozzle, is designed with a relatively low expansion ratio to ensure stable and efficient operation under sea-level conditions [3]. This configuration promotes controlled and symmetric flow separation at the inflection point, which helps mitigate the occurrence of detrimental side loads on the nozzle structure [4]. The second section, known as the extension nozzle, features a higher expansion ratio, enabling improved performance in near-vacuum or high-altitude environments.

Over the past decades, numerous experimental and numerical studies have been devoted to understanding the complex flow behavior within DBNs. Particular emphasis has been placed on design methodologies, given their decisive impact on nozzle performance. The base nozzle contour can be generated using several established approaches, including the truncated ideal contour (TIC) [1], thrust-optimized contour (TOC) [5], and thrust-optimized parabolic (TOP) [6] designs. These methodologies aim to achieve optimal flow expansion while minimizing pressure losses at low altitudes. The extension nozzle, on the other hand, is commonly classified according to its streamwise wall pressure distribution, which may exhibit decreasing, constant, or increasing trends, corresponding to negative (NP), constant (CP), and positive (PP) pressure gradient extensions, respectively [5]. These pressure distributions play a key role in governing the transition between the two operating modes of the DBN [7].

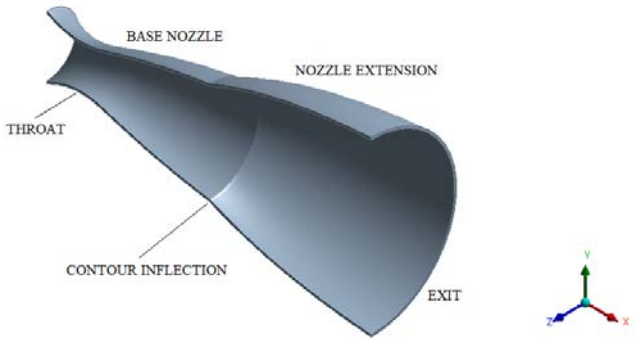

Fig. 1. DBN geometry [1].

In particular, NP extensions are associated with a gradual transition process, often accompanied by significant side-load generation [7]. Conversely, CP and PP extensions

promote faster and more stable transitions, thereby reducing asymmetric flow separation and the resulting structural loads [8]. Owing to these advantages, CP and PP configurations have been the focus of most prior investigations. In addition, several other factors—including geometric parameters such as nozzle length and inflection angle, as well as flow conditions characterized by the Reynolds number and experimental setup—have been identified as having a substantial influence on DBN flow dynamics [5,9,10].

Thrust vectoring represents an advanced control strategy in rocket propulsion, whereby the exhaust jet is deliberately deflected to enhance vehicle maneuverability and ensure accurate attitude and trajectory control. Among the various approaches, fluidic thrust vectoring (FTV) has gained increasing attention as an effective alternative to traditional mechanical systems [11]. Conventional vectoring mechanisms typically rely on movable components, which contribute to increased structural mass—thereby limiting payload capacity—and introduce additional complexity, cost, and maintenance demands. In contrast, FTV achieves jet deflection through fluid-based control techniques without the need for mechanical actuation. This approach not only reduces system weight and mechanical complexity but also offers potential improvements in aerodynamic efficiency and stealth characteristics [11,12]. A wide range of FTV techniques has been explored in the literature, including shock vector control (SVC), co-flow and counter-flow injection, throat sonic-line skewing, and dual-throat nozzles [12]. Although all these approaches rely on secondary flow to manipulate the main exhaust, their underlying mechanisms differ. Among these methods, SVC has received particular attention in recent research due to its relatively simple design and ease of integration into practical propulsion systems.

In SVC, a secondary jet is injected into the divergent section of the nozzle, generating shock waves that deflect the primary flow [12]. Zmijanovic et al. [13] investigated SVC in an axisymmetric conical supersonic nozzle using transverse secondary injection and showed, through air cold-flow experiments and numerical simulations, that even small injection mass-flow rates (~5%) can produce significant lateral forces. Their study also highlighted the critical influence of injector position and geometry on SVC efficiency. The impact of the secondary gas properties on SVC performance has also been studied using various gases, including air, helium, argon, and carbon dioxide [14]. These studies indicated that the product of the specific heat ratio and molecular weight is a key factor influencing vectoring effectiveness.

In the present paper, the shock vector control (SVC) technique applied to an innovative dual-bell nozzle (DBN) is investigated. The paper first presents the design methodology of a novel DBN intended for wind tunnel applications, along with the validation of the proposed configuration and the characterization of the baseline flow without SVC (Section II). Subsequently, the DBN flow under SVC conditions and the corresponding vectoring performance are analyzed (Section III). Finally, the main findings of the study are summarized in the conclusion (Section IV).

II. Dual-Bell Nozzle Design

An in-house code based on the Method of Characteristics (MoC) [15] was developed to generate the DBN contour. The input parameters used in the design are summarized in Table I, while Fig. 2 presents the resulting nozzle profile and its main geometrical characteristics. The base nozzle was designed as a truncated ideal contour (TIC), which ensures shock-free flow expansion [8], whereas the extension nozzle was designed using a constant wall pressure (CP) approach to promote faster and more stable flow transitions [8]. The total length of the DBN is 0.2035 m, with an exit radius of 0.05327 m. The design corresponds to an exit Mach number of 3 and a static pressure of 81671.05 Pa. To validate the proposed design, numerical simulations were performed using computational fluid dynamics (CFD) with the commercial solver ANSYS Fluent 2023 R2 [16]. Fig. 3 shows the wall Mach number distribution along the DBN, comparing MoC predictions with CFD results.

TABLE I. Input Parameters for the MoC Code

Geometrical parameters	Model	2D
	Throat radius R_{th}	0.01 m
	Upstream throat radius R_{tu}	0.03 m
	Downstream throat radius R_{td}	0.03 m
Thermodynamic parameters	Gas	Air
	Specific heat ratio γ	1.4
	Gas constant R	287.55 J/(kg K)
	Stagnation temperature T_0	293 K
	Stagnation pressure P_0	3 MPa

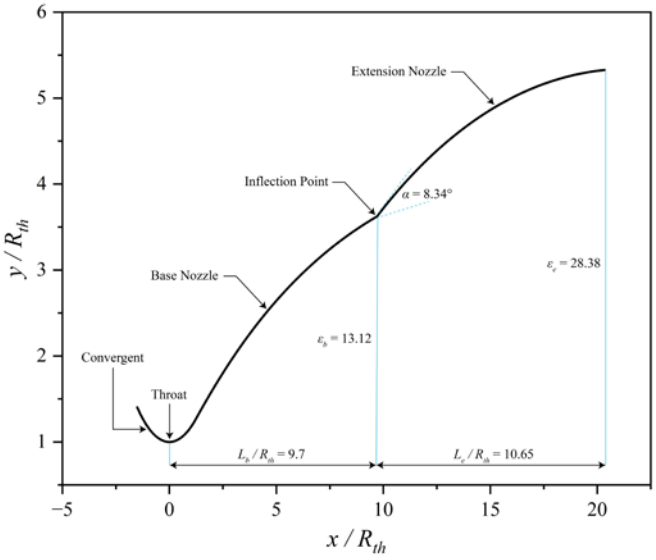

Fig. 2. DBN contour generated using the MoC.

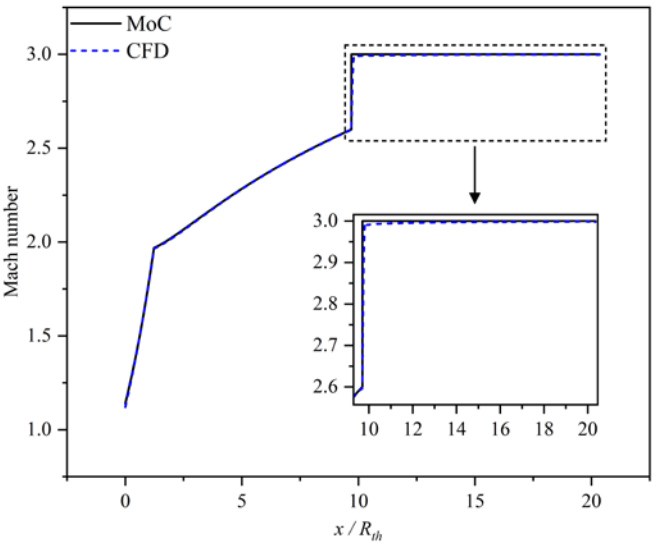

Fig. 3. Wall Mach number distribution along the DBN: comparison between MoC and CFD results.

A close agreement is observed between the two approaches, demonstrating the accuracy and robustness of the developed MoC design method. To analyze the flow characteristics of the DBN under varying operating conditions, the nozzle pressure ratio (NPR), defined as the ratio of stagnation pressure to ambient pressure (P_0/P_a), is considered. CFD simulations were performed for three NPR values: 8.57, 12, and 40. Figure 4 presents the Mach number contours of the DBN without SVC. These conditions correspond to the different operating modes of the nozzle, namely the sea-level mode (Fig. 4(a)), the transition regime (Fig. 4(b)), and the high-altitude mode (Fig. 4(c)). Figure 5 shows the wall static pressure distribution along the DBN, comparing the MoC predictions with CFD results. A good agreement is observed, confirming the validity of the proposed design approach.

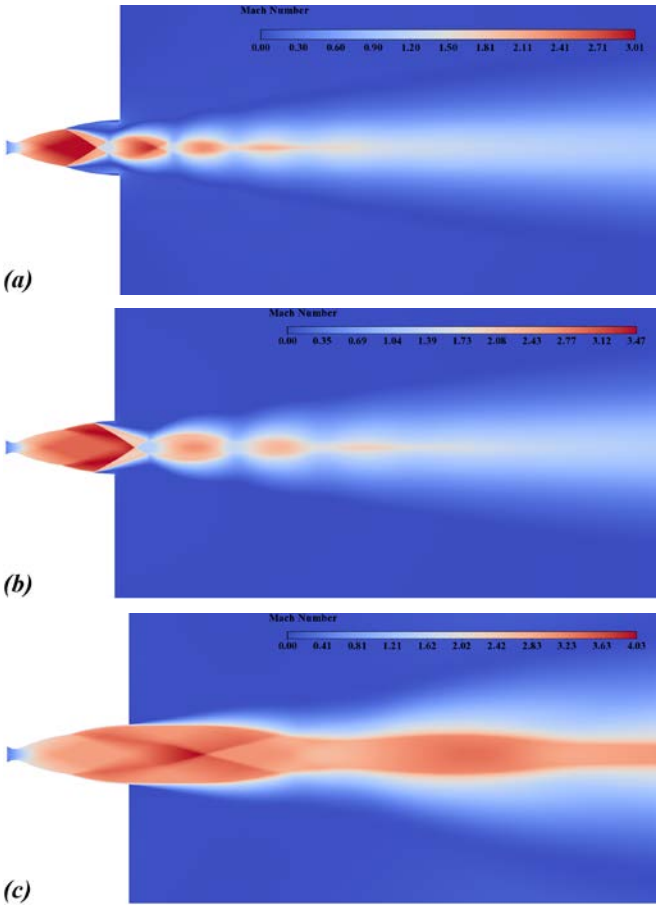

Fig. 4. Flow in the DBN without SVC at varying NPR: (a) NPR = 8.57, (b) NPR = 12, (c) NPR = 40.

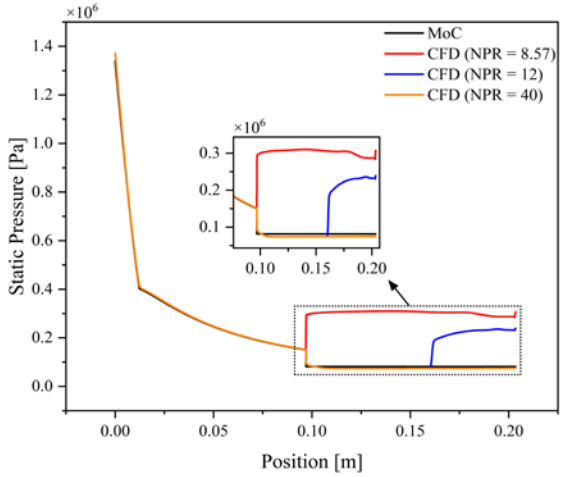

Fig. 5. Wall static pressure distribution along the DBN: comparison between MoC and CFD results.

III. Dual-Bell Nozzle with Shock Vector Control

Fig. 6 presents the numerical Mach number contours of the flow field in the DBN operating with the SVC technique. In this configuration, a secondary jet is injected at the DBN extension to induce deflection of the primary flow. The strength of this injection is characterized by the secondary pressure ratio (SPR), defined as the ratio of the secondary total pressure to the primary total pressure ($P0_j/P_0$). Four SPR values are considered in the present study: 0.3, 0.5, 0.8, and 1. For a fixed nozzle pressure ratio (NPR = 40), it is observed that increasing SPR leads to a greater deflection of the main jet, as evidenced by the increase in the pitch thrust vector angle (δ_p). The injected secondary flow acts as a fluidic obstacle within the primary jet, generating a strong bow shock and inducing an adverse pressure gradient. This pressure rise promotes boundary-layer separation upstream of the injection location, accompanied by the formation of a weak separation shock, as shown in Fig. 7. A recirculation zone develops between the nozzle wall, the separated boundary layer, and the secondary jet plume. This region is characterized by a pair of counter-rotating vortices, identified as the primary upstream vortex (PUV) and the secondary

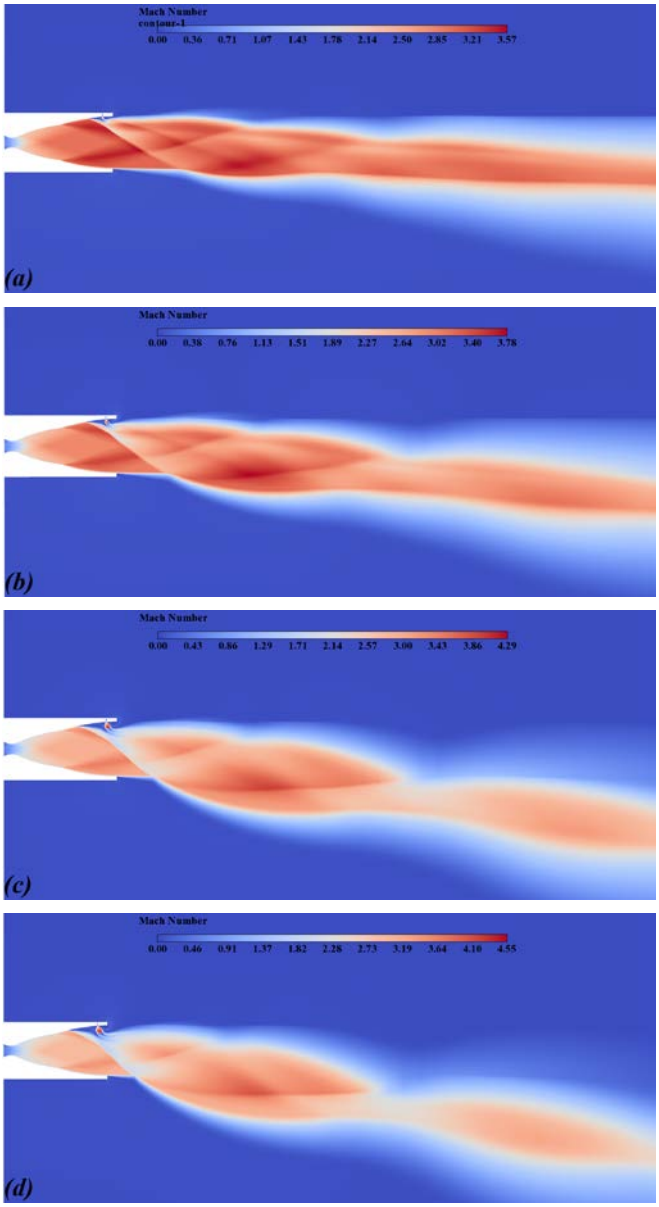

Fig. 6. Flow in the DBN with SVC at varying SPR: (a) SPR = 0.3, (b) SPR = 0.5, (c) SPR = 0.8, (d) SPR = 1.

upstream vortex (SUV), as illustrated in Fig. 8. The PUV forms along the wall and primarily governs the pressure rise associated with flow separation, whereas the SUV, located closer to the injected jet plume, controls the local pressure peak, as depicted in Fig. 9. It is also observed from Fig. 9 that the size of the recirculation zone increases with increasing SPR. Concurrently, the boundary-layer separation point shifts upstream toward the DBN inflection point as SPR increases. Table II summarizes the effect of the SPR on SVC performance at a fixed NPR = 40. Both the δ_p [14] and the thrust vectoring efficiency (η) [14] are observed to increase monotonically with SPR, indicating a substantial enhancement in jet deflection with stronger secondary injection.

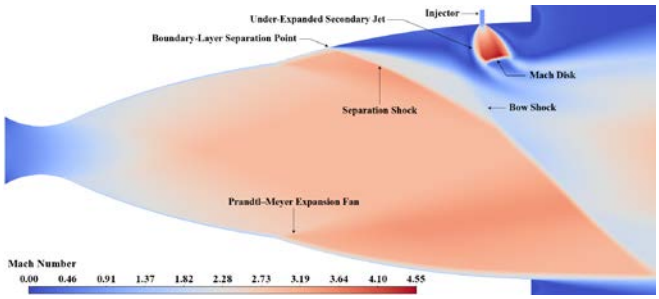

Fig. 7. CFD Mach number contours illustrating flow characteristics and structures in the DBN with SVC.

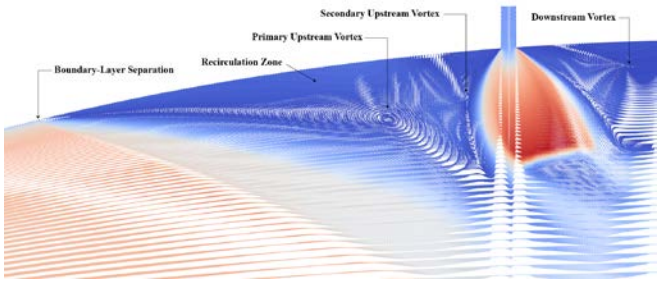

Fig. 8. Flow structures in the vicinity of the injection port.

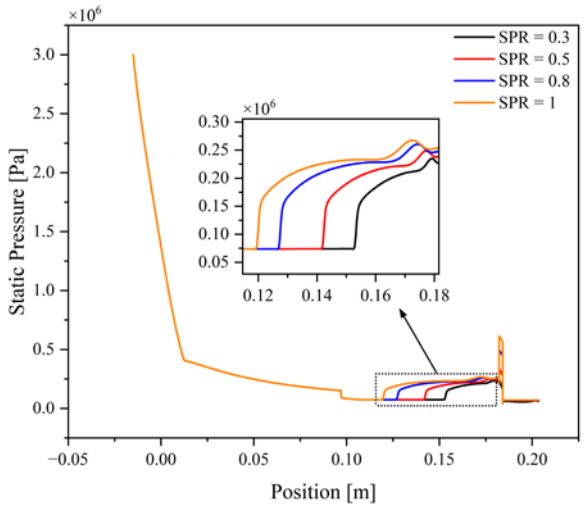

Fig. 9. Wall static pressure distribution along the DBN with SVC obtained from CFD.

TABLE II. SVC PERFORMANCE PARAMETERS

Parameter	Varying SPR at a fixed NPR (NPR = 40)			
	SPR = 0.3	***SPR = 0.5***	***SPR = 0.8***	***SPR = 1***
thrust vector angle (δ_p)	2.37	4.51	7	8.66
thrust vectoring efficiency (η)	0.8	0.91	1.16	1.3

IV. CONCLUSION

The present study investigated the application of the SVC method to DBN rocket propulsion. First, a novel design concept relevant to aerospace applications was proposed and validated through CFD simulations, confirming the accuracy and robustness of the developed MoC code. Subsequently, the integration of an SVC system into the DBN configuration was numerically examined to assess its capability for controlling the maneuverability of a potential launch vehicle. The results demonstrate the effectiveness and potential of this approach for future rocket propulsion.

REFERENCES

[1] A. Tcherak, H. Kbab and A. Haddad, "Proposal of a Novel Dual-Bell Axisymmetric Rocket Propulsive Nozzle Design," *2025 9th International Conference on Mechanical Engineering and Robotics Research (ICMERR)*, Barcelona, Spain, 2025, pp. 198-202, doi: 10.1109/ICMERR64601.2025.10949881.

[2] F. B. Cowles and C. R. Foster, "Experimental study of Gas-Flow separation in overexpanded exhaust nozzles for rocket motors," *NASA Technical Reports Server (NTRS)*, May 09, 1949. http://ntrs.nasa.gov/search.jsp?R=19630039654

[3] R. Stark, C. Génin, D. Schneider, and C. Fromm, "Ariane 5 Performance Optimization using Dual-Bell Nozzle Extension," *Journal of Spacecraft and Rockets*, vol. 53, no. 4, pp. 743–750, Jun. 2016, doi: 10.2514/1.a33363.

[4] H. Kbab, M. Sellam, T. Hamitouche, S. Bergheul, and L. Lagab, "Design and performance evaluation of a dual bell nozzle," *Acta Astronautica*, vol. 130, pp. 52–59, Oct. 2016, doi: 10.1016/j.actaastro.2016.10.015.

[5] Y. Liu and P. Li, "Analysis of the aspiration drag in Dual-Bell nozzles," *International Journal of Aeronautical and Space Sciences*, vol. 24, no. 2, pp. 467–474, Nov. 2022, doi: 10.1007/s42405-022-00541-9.

[6] M. Verma, N. Arya, and A. De, "Investigation of flow characteristics inside a dual bell nozzle with and without film cooling," *Aerospace Science and Technology*, vol. 99, p. 105741, Jan. 2020, doi: 10.1016/j.ast.2020.105741.

[7] F. Nasuti, M. Onofri, and E. Martelli, "Role of wall shape on the transition in axisymmetric Dual-Bell nozzles," *Journal of Propulsion and Power*, vol. 21, no. 2, pp. 243–250, Mar. 2005, doi: 10.2514/1.6524.

[8] C. Genin and R. H. Stark, "Side loads in subscale dual bell nozzles," *Journal of Propulsion and Power*, vol. 27, no. 4, pp. 828–837, Jul. 2011, doi: 10.2514/1.b34170.

[9] S. B. Verma, R. Stark, and O. Haidn, "Reynolds number influence on Dual-Bell transition phenomena," *Journal of Propulsion and Power*, vol. 29, no. 3, pp. 602–609, Mar. 2013, doi: 10.2514/1.b34734.

[10] C. Génin, A. Gernoth, and R. Stark, "Experimental and numerical study of heat flux in dual bell nozzles," *Journal of Propulsion and Power*, vol. 29, no. 1, pp. 21–26, Dec. 2012, doi: 10.2514/1.b34479.

[11] A. K. Das, K. Acharyya, T. K. Mankodi, and U. K. Saha, "Fluidic Thrust Vector Control of Aerospace Vehicles: State-of-the-Art Review and Future Prospects," *Journal of Fluids Engineering*, vol. 145, no. 8, Mar. 2023, doi: 10.1115/1.4062109.

[12] E. Resta, R. Marsilio, and M. Ferlauto, "Thrust vectoring of a fixed axisymmetric supersonic nozzle using the Shock-Vector control method," *Fluids*, vol. 6, no. 12, p. 441, Dec. 2021, doi: 10.3390/fluids6120441.

[13] V. Zmijanovic, V. Lago, M. Sellam, and A. Chpoun, "Thrust shock vector control of an axisymmetric conical supersonic nozzle via secondary transverse gas injection," *Shock Waves*, vol. 24, no. 1, pp. 97–111, Oct. 2013, doi: 10.1007/s00193-013-0479-y.

[14] M. Sellam, V. Zmijanovic, L. Leger, and A. Chpoun, "Assessment of gas thermodynamic characteristics on fluidic thrust vectoring performance: Analytical, experimental and numerical study," *International Journal of Heat and Fluid Flow*, vol. 53, pp. 156–166, Apr. 2015, doi: 10.1016/j.ijheatfluidflow.2015.03.005.

[15] M. J. Zucrow and J. D. Hoffman, Gas Dynamics Volume 2: Multidimensional Flow (John Wiley and Sons, Inc., New York, 1977).

[16] ANSYS, Inc., ANSYS Fluent User's Guide, Release 2023 R2.